Interfacial Reactions in Al-Mg (5083)/SiC*p* Composites during Fabrication and Remelting

W.M. ZHONG, G. L'ESPÉRANCE, and M. SUÉRY

The interfaces of aluminum alloy composites (5083) reinforced by SiC particles (as-received, oxidized 3.04 wt pct and 14.06 wt pct) were studied. The composites were fabricated by compocasting and certain samples were also remelted at 800 °C for 30 minutes. The reaction mechanisms between SiC*p* and liquid Al and between the SiO_2 layer and Al(Mg) are discussed. The crystal boundaries of the MgO (or $MgAl_2O_4$) reaction products are believed to be the diffusion paths (or channels) during the interfacial reactions. A SiO_2 layer, formed by oxidation of the SiC particles prior to their incorporation into the melt, plays an important role in preventing the SiC*p* from being attacked by the matrix. The interfacial reaction products are affected by both the alloy composition and the thickness of the initial SiO_2 layer.

I. INTRODUCTION

INTERFACIAL reactions in metal matrix composites not only affect the interface strength but also the age-hardening behavior of the matrix.[1,2] As reported previously, some interfacial reactions can improve the wettability of the solid reinforcement (*e.g.*, SiC) by the liquid,[3] but sometimes they will cause the reinforcement to be attacked, forming harmful reaction products (*i.e.*, Al_4C_3) around the reinforcement.[4–7] Introducing an oxide layer (SiO_2) on the surface of SiC has been reported to play an important role in preventing SiC from being attacked by liquid Al, improving its wettability and also improving the fracture strain of the composites.[2,8,9] Because the interface reaction in Al/SiC depends on several fabrication parameters (for example, temperature, holding time, atmosphere, and chemical composition of both the aluminum matrix and the SiC reinforcement), the nature of the interface will change with fabrication procedure and composite system.

The reaction between molten Al and SiC particles in the temperature range from 675 °C to 900 °C has been investigated by many authors.[6,10,11,12] From both the points of view of thermodynamics and kinetics, the reaction can take place to yield Al_4C_3 during fabrication by a molten metal route.[6–12] From the studies of Narciso *et al.*[8] and Viala *et al.*,[12] the reaction has been found to proceed *via* a dissolution (of SiC) and renucleation (of Al_4C_3) process. As reported by Lloyd and co-workers[6,10] and Iseki *et al.*,[13] the formation of Al_4C_3 is limited by increasing the Si content of molten Al.

A chemical interaction between molten Al and SiO_2 was observed by Narciso *et al.*[8] and Brondyke[14] at 700 °C to 900 °C, forming Al_2O_3 and Si. The reaction rate was believed to be controlled by the diffusion of Al and Si through the newly formed Al_2O_3 layer. Legoux and co-workers[5,9] have extensively studied the reaction between the SiO_2 layer on SiC*p* and Al alloys (containing 0.3, 1, and 5 wt pct Mg). $MgAl_2O_4$ was found to be the reaction product in the materials with 0.3 and 1 wt pct Mg, whereas a mixture of $MgAl_2O_4$-MgO fine crystals was the reaction product in the materials made with 5 wt pct Mg. Metallic Al channels were shown to be the diffusion path through the oxide layer for incoming Mg and outgoing Si. Stephenson *et al.*[15] found, experimentally, that the reaction tendency and kinetics of Mg and SiO_2 are several times higher than that of Al and SiO_2 at 670 °C to 800 °C; however, they did not discuss the diffusion paths. Jin and Lloyd,[16] in studying the reaction between pure Al-Mg alloys and Al_2O_3 particles, found that the reaction rate decreased for higher Mg contents (>5 wt pct) because of the small size of the reaction product formed ($MgAl_2O_4$).

In this work, the reaction mechanisms between SiC particles covered by a SiO_2 layer and a commercial alloy containing a large amount of Mg (5083 alloy) are investigated in detail. Of particular interest are the effects of the alloy composition, the fabrication parameters, and the nature of SiC particles on the interfacial reaction. The role of the SiO_2 layer in protecting SiC in 5083/SiC*p* composites has also been investigated. The 5083 aluminum alloy is a solution-hardening alloy. It has moderate strength and good corrosion resistance. It has a potential for superplastic deformation. The mechanical properties and the high-temperature deformation behavior of the composites have been reported elsewhere.[17] A study of the effects of the thermomechanical processing of the composites and the interfacial reactions on the strengthening and fracture mechanisms will also be reported elsewhere.

II. EXPERIMENTAL PROCEDURES

A modified compocasting technique was used to fabricate the composites. The 5083-Al alloy was first heated to the semisolid state in the temperature range from 600 °C to 640 °C. The reinforcing particles were then incorporated into the vigorously agitated alloy. Approximately 5 minutes were required to add all the particles. Finally, the alloy was completely remelted at 720 °C for 5 minutes and solidified under a pressure of 100 MPa.[2] The particles used were either in an as-received condition (from PRESI, France) or

W.M. ZHONG, Postdoctoral Student, and G. L'ESPÉRANCE, Professor, are with the Materials Engineering Department, Ecole Polytechnique, Montreal, PQ, H3C 3A7 Canada. M. SUÉRY, Professor, is with the National Polytechnique Institute, Grenoble, 38402 St. Martin d'Heres Cedex, France.

Manuscript submitted March 17, 1994.

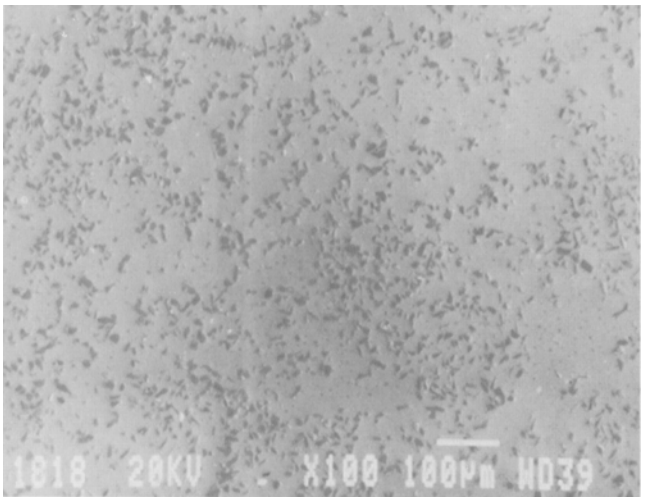

Fig. 1—Distribution of SiC*p* (ARS, 5083/SiC*p*, as-cast).

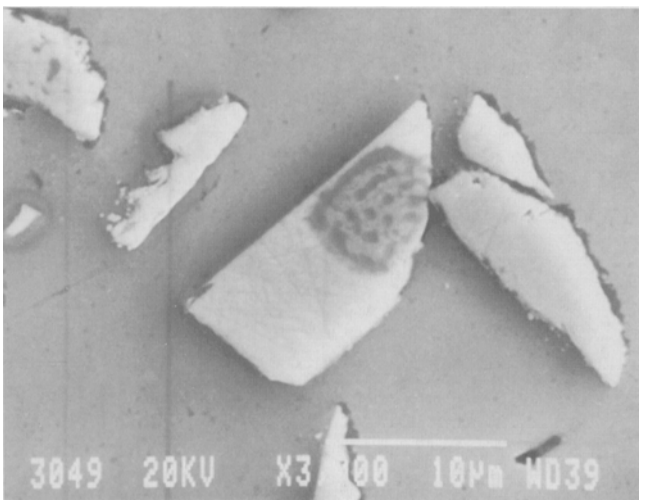

Fig. 2—SiC*p* boundary is clear, no reaction product is seen at the interface (ARS).

in an artificially oxidized condition. Oxidation was carried out in air at 1100 °C for two different times (about 1 and 12 hours) using a SiC crucible heated with an induction furnace. The SiO_2 layer formed in this way was continuous and the amount of SiO_2 determined by wet chemical analysis was 3.04 and 14.06 wt pct of the particle weight for oxidation times of 1 and 12 hours, respectively. A total of 15 vol pct of SiC*p* was used (with a diameter of 13 μm). The remelting experiments were performed in an induction furnace using a small graphite crucible under Ar atmosphere. The samples were reheated to 800 °C and held for 30 minutes. The composition of the alloy used is 4.1 wt pct Mg-0.56 wt pct Mn-0.12 wt pct Cr-0.19 wt pct Fe-0.15 wt pct Si-0.04 wt pct Cu-0.02 wt pct Ti-(bal.) Al.

All the internal acronyms used in this article were designated to indicate the state of the particles prior to their incorporation into the composites and the state of the composites (*i.e.*, as-cast or remelted). For example, sample AOX14 means that the sample was as-cast (A) and the particles were oxidized (OX) 14 wt pct, and sample ROX14 means that the same composite was remelted (R).

Scanning electron microscopes (SEM) (JEOL-840, JEOL-820) and transmission electron microscopes (CM30-PHILIPS, JEOL-2000FX) were used. The interface microstructure was examined by using bright-field (BF) images, dark-field (DF) images, selected area diffraction (SAD), microdiffraction, and electron energy loss and energy dispersive X-ray spectroscopies (EELS and EDS). The TEM thin foils were prepared by ion milling at 15 deg with a voltage of 5 kV after mechanical polishing and dimpling.

III. EXPERIMENTAL RESULTS

A. *5083/SiCp Composites (As-Received SiCp, As-Cast Composites, (ARS))*

Figures 1 and 2 are SEM micrographs showing the distribution of the SiC particles in the composites and the interface between the SiC and the matrix. As shown in Figure 1, the distribution of SiC*p* is macroscopically uniform. At a magnification of 3000 times, interface reaction products and porosity are not observed.

Figure 3(a) shows a TEM micrograph in which the SiC particle is not attacked by the matrix. Figure 3(b) is the corresponding EDS line profile at the matrix/SiC*p* interface. No Mg is found inside the SiC particle, as shown by the curve which represents the true Mg concentration profile near the interface. The Mg apparently detected inside the SiC particle is caused by electron beam broadening, as confirmed by a deconvolution technique in which electron beam broadening and the expected true Mg concentration profile (the solid curve in Figure 3(b)) are convoluted to yield the experimental profile.[18] $C_{\text{apr-measured}}$ and $C_{\text{apr-calculated}}$ represent the measured and the convoluted apparent Mg concentration. The Mg and O are found at high levels (as high as 17 wt pct Mg) at the interface. Figure 4 is a higher magnification TEM micrograph which shows that fine MgO crystals, as confirmed from the indexation of the SAD pattern, have formed near the SiC particle. The thickness of the MgO layer can be larger than 50 nm but is typically in the 10 to 30 nm range. Occasionally, penetration of the matrix into a SiC particle along a crystal defect can be observed. A Cr-, Mn-, Fe-rich phase such as $(Cr,Mn,Fe)_3SiAl_{12}$ is frequently found near the SiC particle. This phase is not associated with interfacial reactions but is a normal inclusion in 5083 aluminum alloy. Mg_2Si is also observed in the matrix and near SiC particles.

B. *5080/SiCp Composites (As-Received SiCp, Remelted at 800 °C for 30 minutes, (RMS))*

After remelting of the composites, SiC*p* particles are attacked heavily (Figure 5). From the SEM micrograph, we can see that a large number of Mg_2Si particles are formed in the matrix and around the SiC particles.

The TEM image in Figure 6(a) shows an attacked SiC particle where Al_4C_3 is formed. Figure 6(b) is a SAD pattern obtained from Al_4C_3. At some places, MgO crystals (see arrows in Figure 7(a)), which may be formed during fabrication of the composites, are still found at the original interface of matrix/SiC*p*. Al_4C_3 is observed behind the MgO layer as a result of the attack of SiC during remelting. At the same time, Mg_2Si is found in the matrix near the MgO reaction zone. Figure 7(b) is the corresponding SAD (annular) pattern from MgO crystals. These results indicate

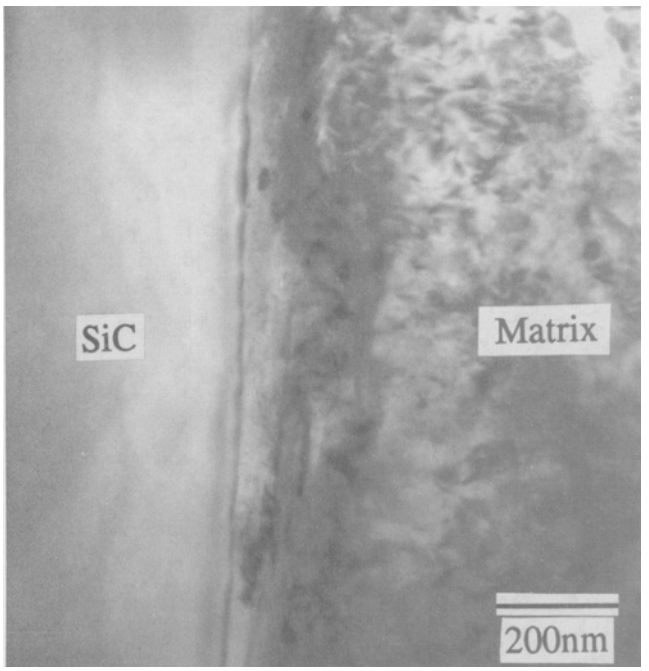

(*a*)

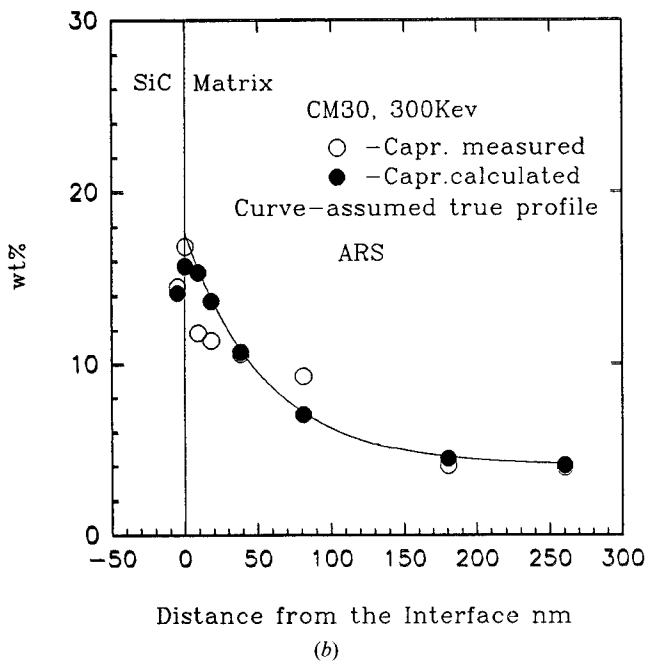

(*b*)

Fig. 3—(*a*) TEM image of the interface of matrix/SiC*p* (ARS). (*b*) EDS line-profile at matrix/SiC*p* interface (ARS).

that in as-cast materials MgO is not formed at every matrix/SiC*p* interface and that the oxide layer on the as-received SiC particles is not uniform. After remelting, Mg was not detected in the matrix using EDS.

C. *5083/SiCp Composites (SiCp Oxidized 3.04 wt pct, As-Cast, (AOX3))*

A reaction layer consisting mainly of fine MgO crystals is shown by TEM images in this sample (Figures 8(a) through (c)). The sizes of MgO particles are about 5 to 20 nm. As shown by the EDS line profile and the EDS spectrum (Figures 9 (a) and (b)), Mg and O contents are high in the reaction zone. The thickness of the reaction zone is about 100 to 200 nm on average. Inside the reaction zone, the SiC*p* boundary is clear and straight. There is no evidence of SiC*p* attack. Mg_2Si is found near the reaction zone in the matrix. $(Mn,Fe)Al_6$ and $(Cr,Mn,Fe)_3\ SiAl_{12}$ are also found in the sample. There is about 2.5 to 3 wt pct Mg remaining in the matrix measured using EDS.

D. *5083/SiCp Composites (SiCp Oxidized 3.04 wt pct, Remelted at 800 °C for 30 Minutes, (ROX3))*

After remelting, as shown in Figures 10(a) and (b), most of the SiC particles still have clear, smooth boundaries indicating no attack by the matrix. Mg_2Si (dark phase) is found around the particles. A few particles with serrated boundaries can be seen; they were attacked at some places (Figure 11). As shown in Figures 10 and 12, the matrix/SiC*p* interfaces are still rich in Mg and O. By TEM observation, the reaction zone around SiC*p* still consists of fine MgO crystals, as shown in Figures 13(a) through (c). Figure 13(d) is an EELS spectrum obtained from the reaction zone, which shows a sharp Mg peak caused by the presence of MgO crystals, as indicated from a comparison with an EELS spectrum of a pure MgO crystal. Metallic Al present in the reaction zone is identified by the relatively smooth Al peak on the EELS spectrum.[5] Mg_2Si is also observed near the reaction zone in the matrix, identified by SAD in TEM observation.

E. *5083/SiCp Composites (SiCp Oxidized 14.06 wt pct, As-Cast, (AOX14))*

X-ray maps in Figure 14(a) reveal the presence of Mg, O, and Al in the reaction zone. The interface reaction zone is also quite evident in the SEM image (Figure 14(b)). Mg_2Si (D, dark phase) and some $(Cr,Mn,Fe)_3SiAl_{12}$ (B, bright phase) are found in the matrix near the SiC*p*. The thickness of the reaction zone is about 500 to 800 nm.

TEM micrographs (Figures 15(a) and (b)) show that the reaction layer consists mainly of fine MgO crystals, confirmed by the high intensity of the MgO diffraction rings. Diffraction spots, $(111)Mg_2Si$, $(012)Al_2O_3$, $(111)MgAl_2O_4$, and $(100)SiO_2$, also appear occasionally in the SAD patterns obtained by using different tilt angles, which can be used to unambiguously identify the presence of these phases in the reaction zone. Figure 16(a) shows an EDS line profile at the matrix/SiC*p* interface, which illustrates the distribution of Mg, O, and Al. Figure 16(b) is an EDS spectrum obtained from the reaction zone. The SiC particles have not been attacked at all. The Mg_2Si in the matrix and near the SiC*p* is a product of solidification. Silicon is produced by the reaction between SiO_2 and Mg or Al. In comparison to the AOX3 sample (with 3.04 wt pct SiO_2 layer), the reaction products are more complex in the reaction zone of the AOX14 sample (with 14.06 wt pct SiO_2 layer). About 0.5 to 1 wt pct Mg was measured remaining in the matrix.

F. *5083/SiCp Composites (SiCp Oxidized 14.06 wt pct, Remelted at 800 °C for 30 Minutes, (ROX14))*

In the ROX14 samples (with SiC*p* oxidized 14.06 wt pct, remelted), the proportion of $MgAl_2O_4$ in the reaction zone

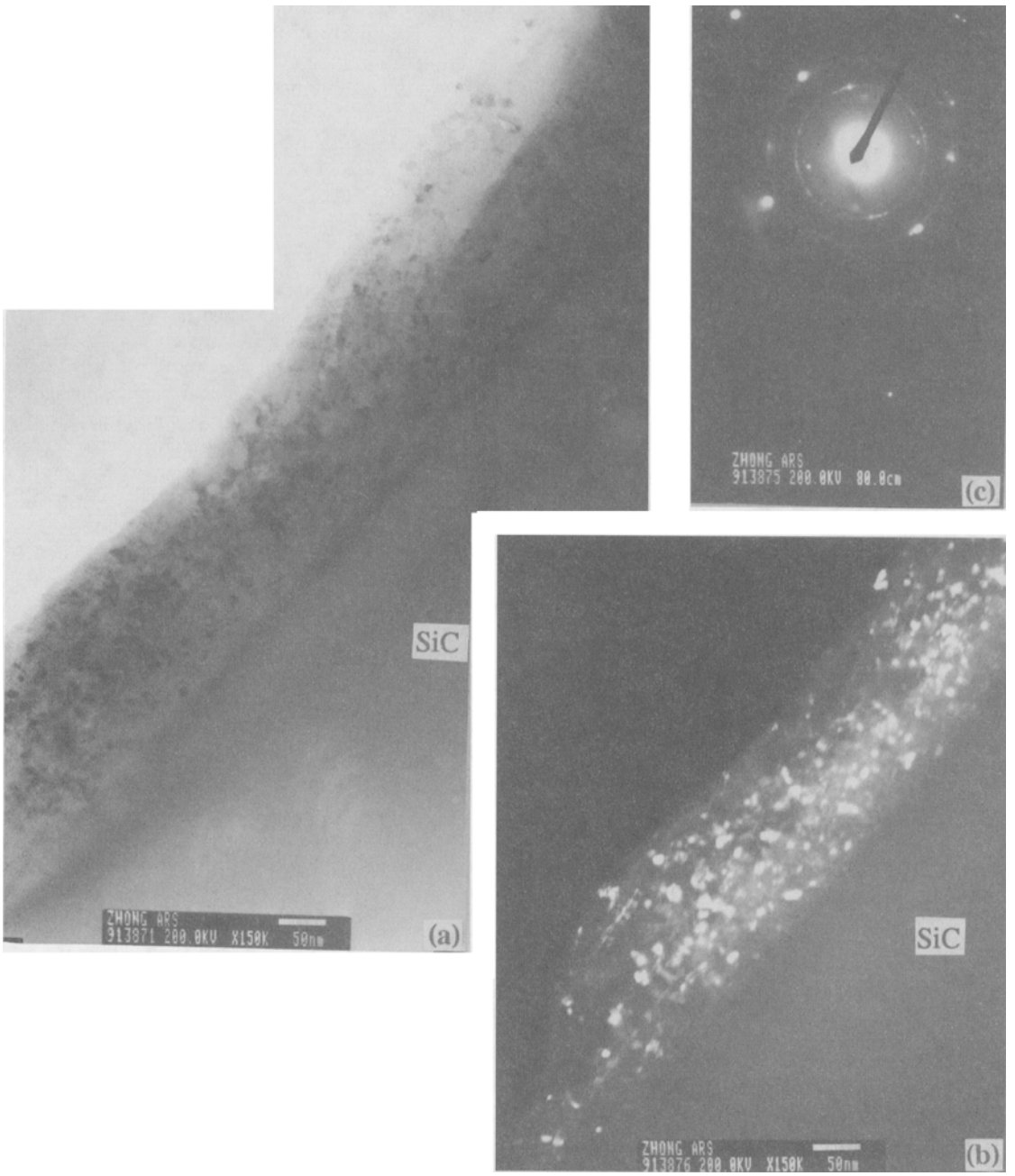

Fig. 4—Small MgO crystals are observed at the interface: (*a*) TEM BF image, (*b*) DF image, (*c*) SAD pattern from reaction zone (MgO size 5 to 10 nm, ARS).

has increased after remelting (Figure 17). Figure 17(b) shows a very strong (111) diffraction ring from $MgAl_2O_4$. Large Si and Mg_2Si phases (>1 μm) are found near the reaction zone in the matrix, as shown in Figure 17(a). $MgAl_2O_4$ crystals, with a size in the range of 0.5 to 1 μm, are also found occasionally just outside the reaction zone (Figure 17(a) and the corresponding diffraction pattern in Figure 17(c)). Figures 18(a) and (b) are the TEM BF and DF images (obtained with the (111) spinel diffraction spots). The crystal size in the reaction zone appears slightly larger than that in as-cast composites. Figures 18(c) and (d) are the diffraction patterns obtained from pure MgO and $MgAl_2O_4$ standards, respectively. Diffraction from $(111)_{spinel}$ with a d spacing of 0.466 nm and from $(220)_{spinel}$ with d = 0.285 nm can be used to identify the presence of $MgAl_2O_4$. Figure 19 is the EDS line profile of Mg, O, and Al at the matrix/SiC*p* interface. No Mg remains in the matrix after remelting.

As can be seen, the reaction products at the interfaces of the composites with the 3.04 wt pct SiO_2 layer are different from those with the 14.06 wt pct SiO_2 layer. In the latter case, a thicker SiO_2 layer increases the probability of $MgAl_2O_4$ formation.

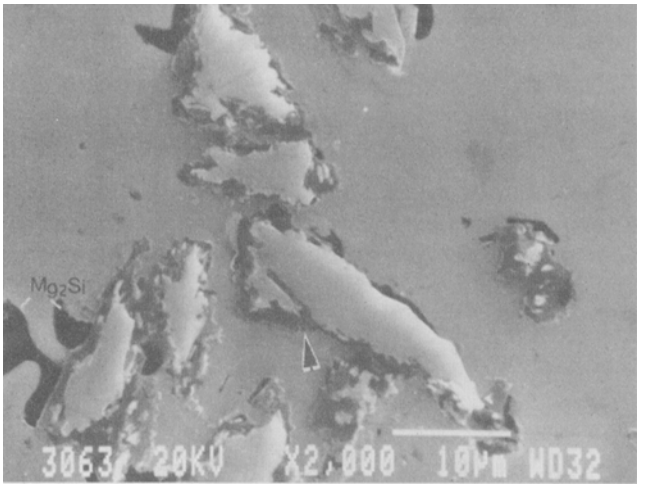

Fig. 5—SiC*p* attacked by matrix (RMS, 5083/SiC*p*, remelted at 800 °C for 30 min).

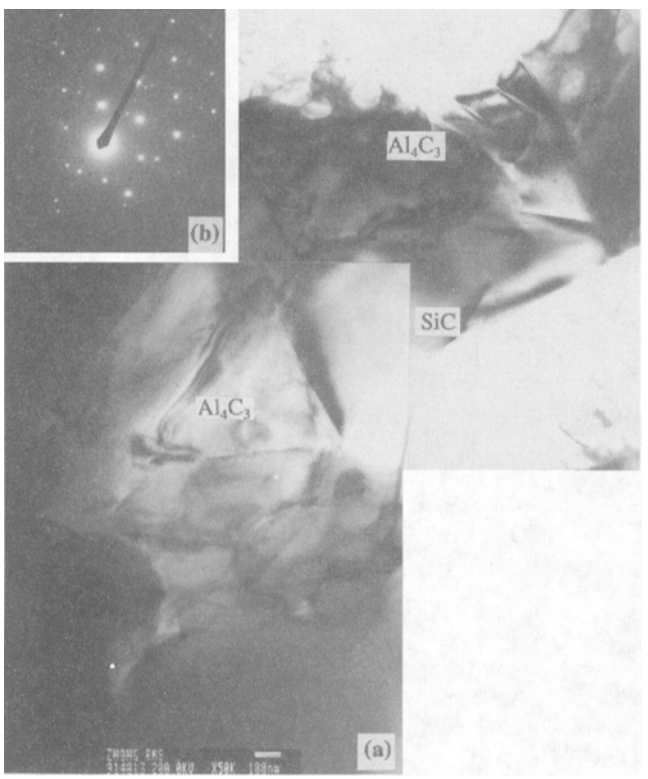

Fig. 6—(*a*) TEM BF image, the morphology of the attacked SiC*p* (RMS). (*b*) SAD patterns of B[210]Al_4C_3.

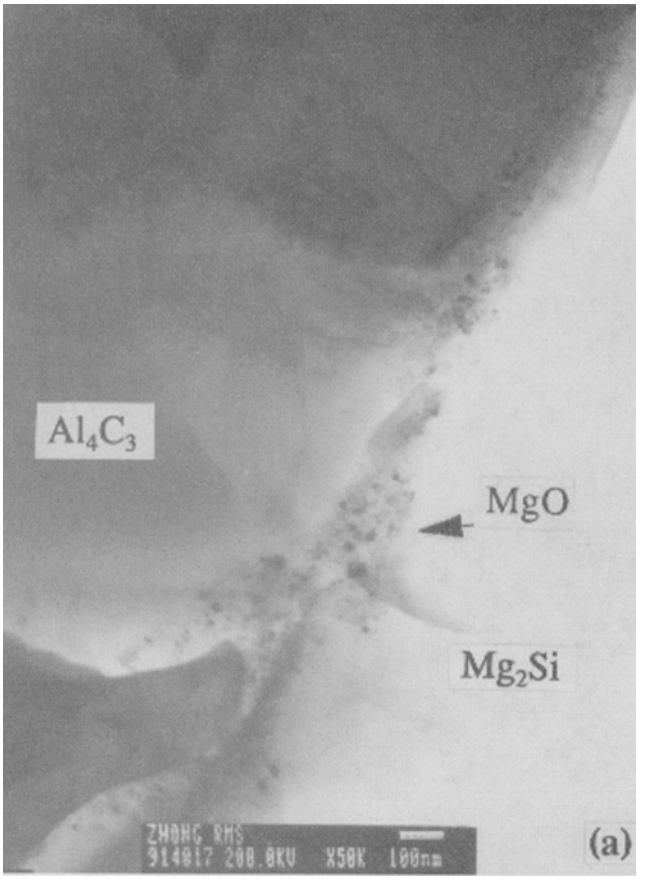

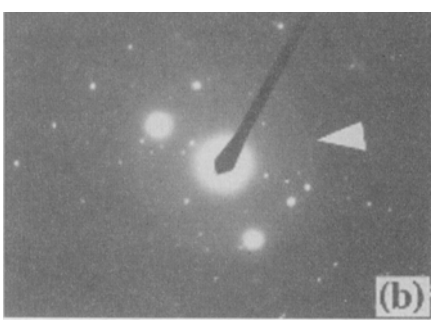

Fig. 7—(*a*) MgO crystals are observed at the original interface in front of Al_4C_3 (RMS). (*b*) SAD patterns of MgO polycrystal.

IV. DISCUSSION

A. *The Reaction Mechanism between Liquid Al and SiC Particles*

The reaction between SiC*p* and liquid Al is believed to include several steps including the following:[19,20]

(a) chemical reaction (dissolution) of SiC*p* with molten Al;
(b) diffusion of Si and C atoms away from the SiC*p* surface into the molten Al pool;
(c) formation of compounds when the Al and C concentrations or the Si and C concentrations exceed the equilibrium constants of Al_4C_3 or SiC; and
(d) further precipitation of compounds on cooling due to a decrease in solubility.

The dissolution kinetics of SiC*p* in Al have been suggested to be the rate-determining step in the Al/SiC interfacial reaction during manufacture of composites.[19] As mentioned previously, increasing the amount of Si in the matrix can reduce the dissolution of SiC and prevent the formation of Al_4C_3.[6,11] As shown by Lloyd,[21] the reaction rate is very low in the fabrication temperature range from 650 °C to 750 °C (after holding for 2 hours at 750 °C, no

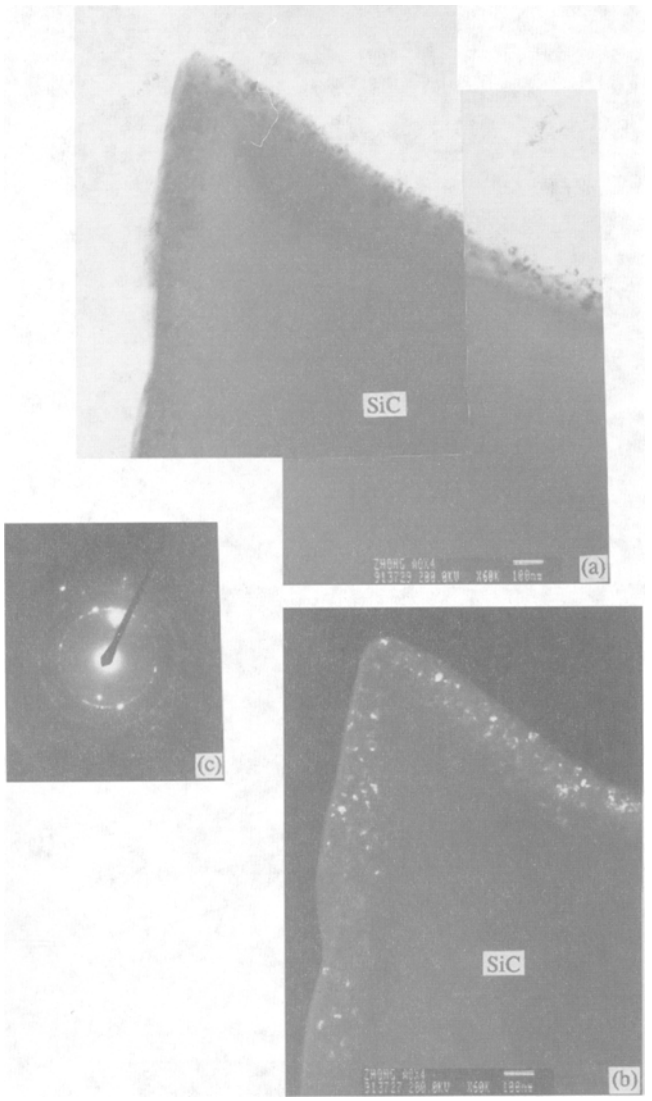

Fig. 8—(*a*) TEM BF image, (*b*) DF image by (111)MgO, and (*c*) SAD pattern of MgO obtained from the reaction zone (AOX3).

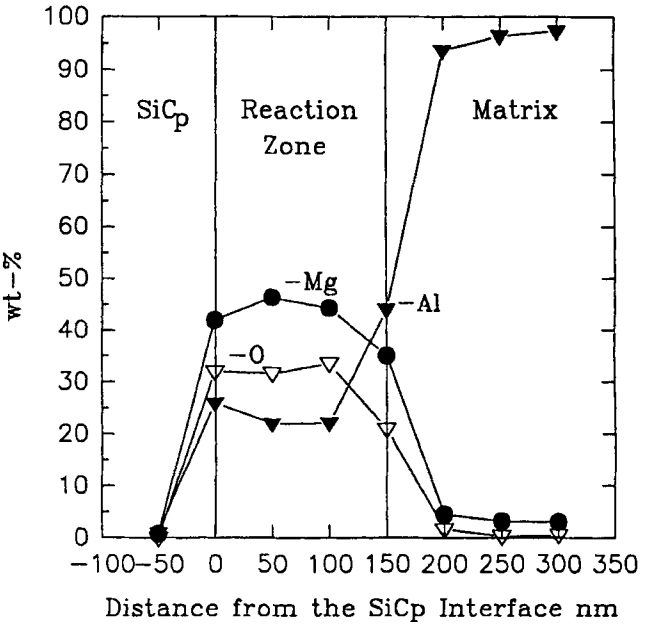

(*a*)

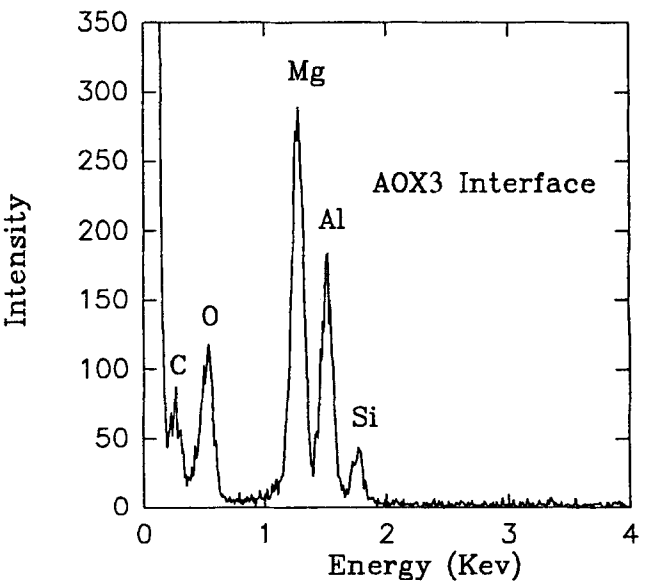

(*b*)

Fig. 9—(*a*) EDS line profile for AOX3. (*b*) EDS spectrum in the reaction zone.

attack was observed in the A356 (7 wt pct Si) alloy). Usually, 7 to 15 wt pct of Si is necessary to prevent the reaction.[6,11,12,19,21] Since the matrix of the composites studied in this work contains only 0.15 wt pct of Si, SiC is expected not to be stable in contact with the liquid Al. From our experimental results, we find that the dissolution of the SiC*p* is not uniform, as shown from the preferentially attacked channels and the serrated morphology of the attacked SiC particles. The dissolution of the SiC*p* seems to be a preferential process (*e.g.*, along crystal defects or along some low index crystal planes).

Because the solubility of [C] in liquid Al is very low at temperatures from 660 °C to 800 °C, the threshold carbon activity values for Al_4C_3 formation are small. The carbon atoms that go into solution will react almost immediately with Al to form Al_4C_3.[22] With the dissolution of SiC, the Al_4C_3 grows and Si will diffuse into the melt around the Al_4C_3. Therefore, at the beginning, the dissolution of the SiC*p* into the molten Al will control the Al/SiC*p* interface reaction. With increasing time, a layer of Al_4C_3 may form around the SiC particle, similar to the observation of Iseki.[13] The Al_4C_3 layer may act as a diffusion barrier for the diffusion of Si, C, and Al; thus, further reactions will be affected by the diffusion process, although other diffusion paths, like crystal boundaries and defects, are also available.

B. *Enrichment of Mg at the Al (Mg) Alloy/Reinforcement Interface*

In many Al (Mg) matrix composites, segregation of Mg at the matrix/reinforcement interface is frequently observed.[2,9,23,24,25] In 5083/SiC*p* as-cast materials, segregation of Mg is also found. This may have several causes. First, just as in Al-Mg alloys,[26] Mg can segregate at the grain boundaries and free surfaces. This segregation is governed by thermodynamic factors related to the decrease of the grain boundary energy, interface energy, or surface energy.

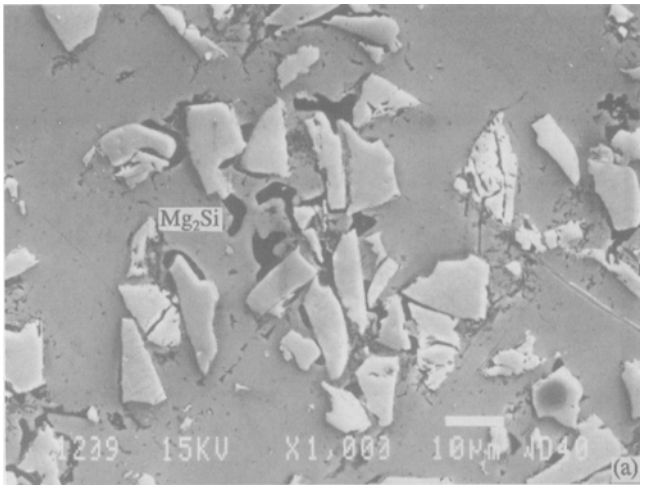

(*b*)

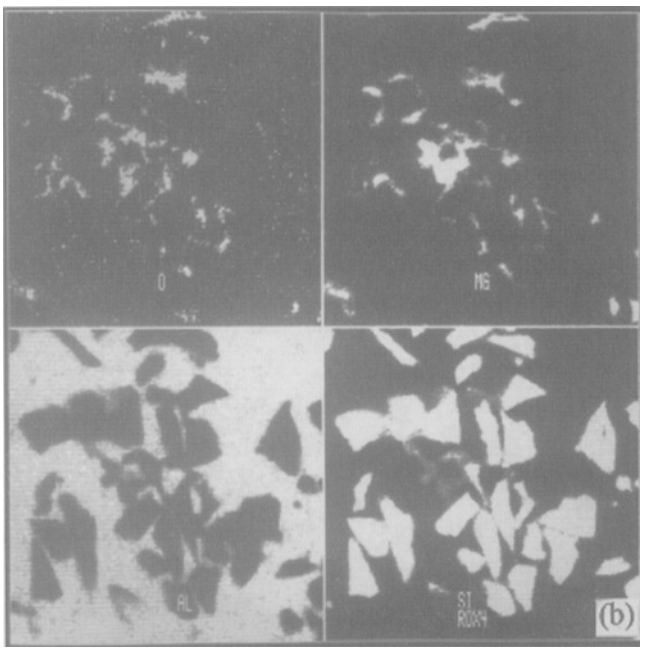

(*b*)

Fig. 10—(*a*) and (*b*) SEM X-ray maps of the interfaces enriched in Mg and O (ROX3).

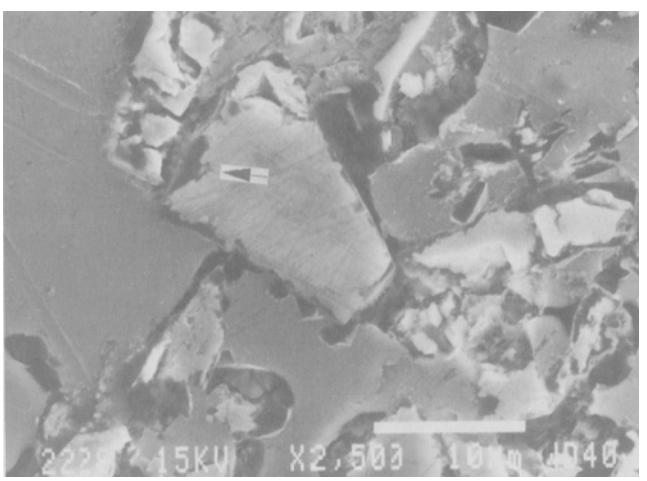

Fig. 11—After remelting, some particles are attacked (ROX3).

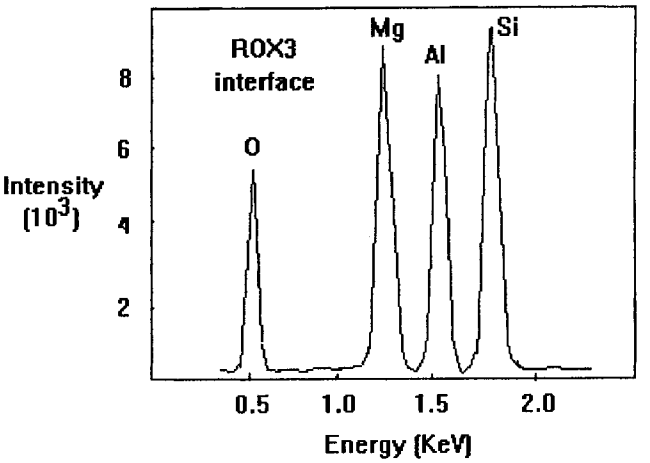

Fig. 12—EDS spectrum obtained from the matrix/Si*Cp* interface (ROX3).

For example, in a quenched sample, nonequilibrium segregation is established by vacancy drag of solutes as defects migrate to the sinks (grain boundaries).[26] In composites, the interface of matrix/reinforcement is also a good sink for the solute atoms during rapid cooling.

Second, segregation of Mg is caused by the interfacial reaction of Mg with the SiO_2 layer on the Si*Cp* surface, or with the oxygen trapped during the fabrication process, to form MgO or $MgAl_2O_4$ oxides.[2,12,27] These reactions can improve the wettability and form a diffusion barrier for reaction between liquid Al and Si*Cp*.[1,28]

Third, nucleation of the primary solid does not occur initially on the surface of the reinforcement during solidification. In the case of an alloy, the solid phase will avoid the reinforcement as it grows. Consequently, the last portion of the metal to solidify will be located close to or at the matrix/reinforcement interface with the solutes pushed to the interface by the liquid/solid front. Therefore, enrichment in the solutes (Mg) is observed near the interface.[18,20,29]

C. *Reaction Mechanism of the SiO_2 Layer with Liquid Al-Mg Alloy*

Reactions between Mg and SiO_2 layer can form MgO or $MgAl_2O_4$, MgO being formed more easily with high Mg content in matrix.[5,9] That is

$$SiO_2 + 2Mg = 2MgO + Si \quad [1]$$

$$2SiO_2 + Mg + 2Al = MgAl_2O_4 + 2Si \quad [2]$$

After the first layer of MgO or spinel is formed, for the reaction to continue, Mg, Al, and the released Si must diffuse through the reaction layer. As the bulk diffusion coefficients of these elements in oxides at temperatures of 700 °C to 800 °C are very small[9,30] and since the reaction products are extremely fine crystals, crystal boundary diffusion must play an important role. Horvath[31] studied diffusion in nanocrystalline materials (crystal size about 10 nm). Owing to the enormous interface area in the material, the diffusion coefficient is many orders of magnitude higher than the lattice bulk diffusion coefficient. Bokstein[32] found that the grain boundary or phase boundary diffusion coefficient in Ti alloys is 5 to 6 orders of magnitude higher than that of its volume diffusion. Formation of $MgAl_2O_4$ from SiO_2

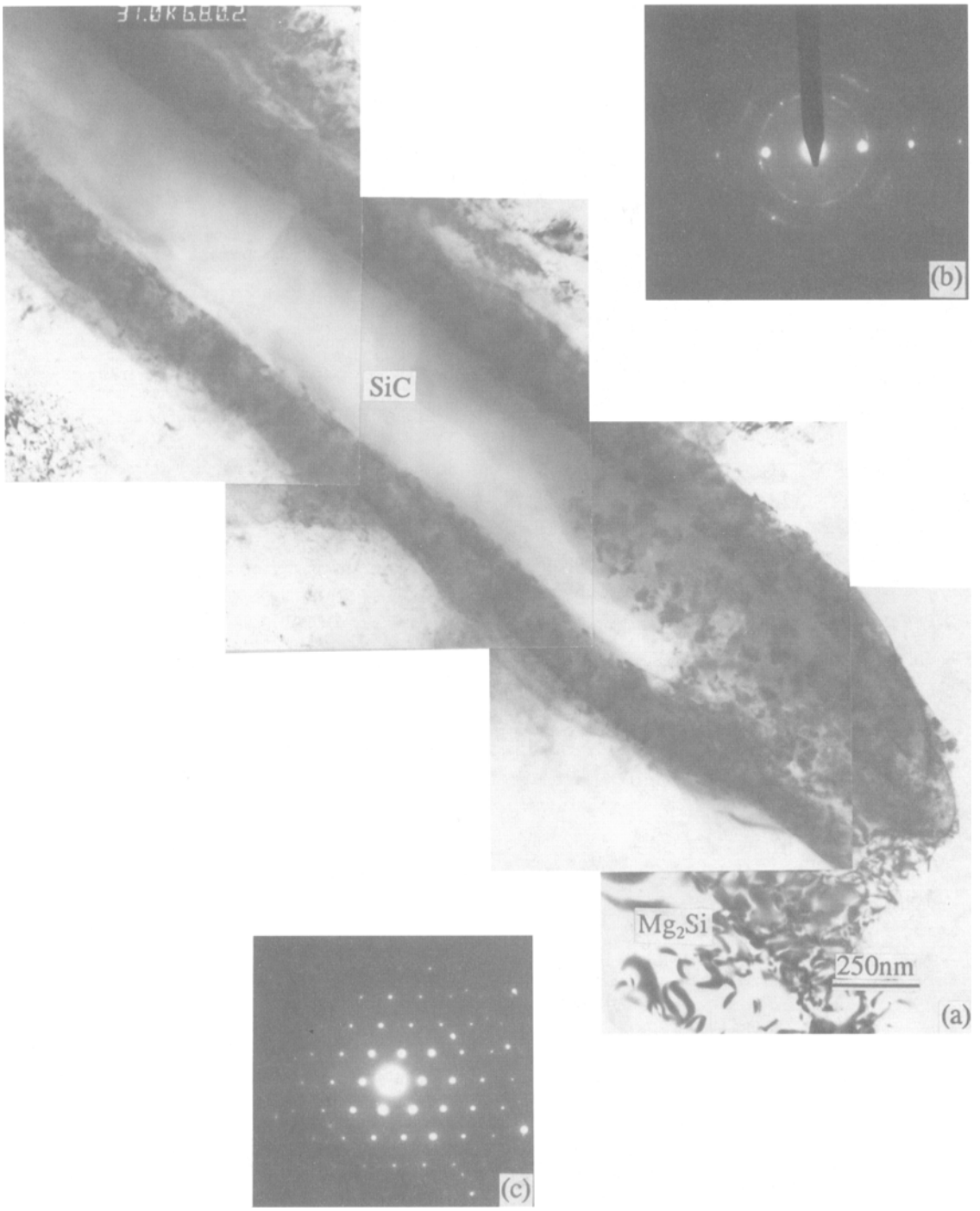

Fig. 13—(*a*) TEM BF image of ROX3. (*b*) SAD pattern of MgO. (*c*) Mg_2Si is found near SiC*p*, B[110]Mg_2Si.

will cause a 27 pct volume contraction, and formation of MgO will cause a 13.6 pct volume contraction. Due to this contraction, there will be gaps between the newly formed crystals or between the newly formed crystals and the rest of the SiO_2. Liquid Al and Mg infiltrate into these gaps and form so-called "diffusion channels," as Legoux, *et al.*[9] suggested. Released Si will diffuse through these channels into the liquid and may form Mg_2Si with the Mg in matrix; that is

$$Si + 2Mg = Mg_2Si \qquad [3]$$

The reaction between Mg (or Al) and SiO_2, during the fabrication of the composites, becomes kinetically possible because of the diffusion channels. However, our experimental results have shown that the attack of SiC by molten Al is decreased with increasing thickness of the SiO_2 layer during remelting. The reason is that the newly formed MgO or spinel crystals in the reaction zone decrease the effective exposed surface of the SiC particle to the molten Al and form a diffusion barrier for the incoming Al. In as-cast composites, the SiO_2 layer on SiC surface may also delay direct contact of molten Al with the SiC particles during incorporation, especially when the SiO_2 layer is thick. Of course, because of the large volume contraction in forming

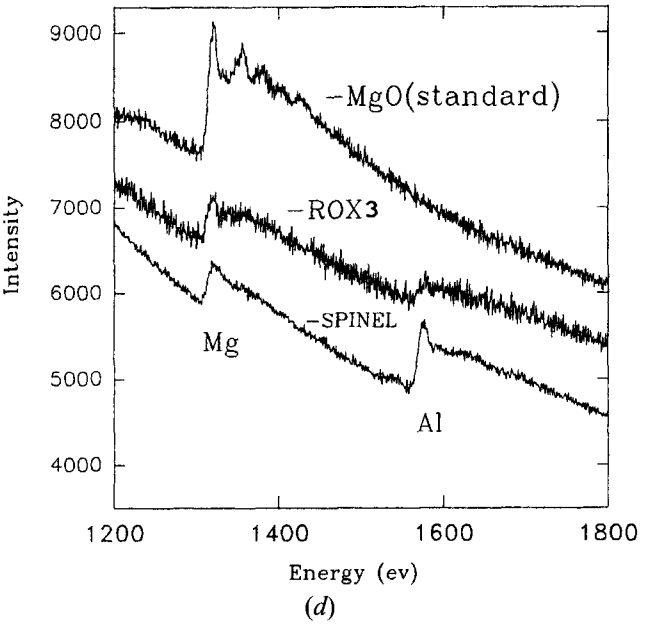

(*d*)

Fig. 13—(*d*) PEELS spectra obtained from the reaction zone (ROX3), pure spinel, and MgO standards.

MgO (13.6 pct) or spinel (27 pct) crystals from SiO_2, the protecting role of the reaction zone should be less important compared to the reaction between Mg and Al_2O_3 particles.[33] The reaction between Mg and Al_2O_3, in which the protecting role of the newly formed MgO or spinel crystals is more pronounced because of the large volume expansion (30 pct for MgO and 15 pct for $MgAl_2O_4$), makes the diffusion channels become very narrow during the reaction.[33] It is quite possible that forming MgO in the reaction zone will protect SiC better than forming $MgAl_2O_4$ does, owing to the smaller volume contraction in forming MgO crystals and the lower diffusivity in MgO crystal. Thus, SiC will be protected better with a higher Mg content in the matrix because the probability of forming MgO increases with increasing Mg content, while the thickness of the SiO_2 layer is constant.

As discussed earlier, MgO is the main interfacial reaction product in the ROX3 sample (3.04 wt pct oxidized, remelted), whereas $MgAl_2O_4$ is the main reaction product in the ROX14 sample (14.06 wt pct oxidized, remelted) and MgO is the main reaction product in the as-cast composites (AOX3 and AOX14) reinforced by the two different particles. This difference can be explained as follows. Although both AOX14 and AOX3 (as-cast) materials have the same original Mg contents, the "dynamic" concentration in the matrix will be affected by the quantity of SiO_2 available on the surface of the particles. For the materials with a thicker SiO_2 layer, the Mg concentration at the beginning of the reaction will be quite different from that near the end of the reaction. It is known that MgO forms more readily with higher Mg contents, as discussed previously.[5,24,29,34] In the AOX3 sample, because the SiO_2 layer is thin, the interfacial reaction consumes only a small amount of Mg (consuming about 1 wt pct according to our measurements and 0.96 wt pct as calculated from Reactions [1] and [3]). In addition, the semisolid processing during compocasting may increase the actual Mg content in the remaining liquid. Therefore, MgO is the main reaction product even at the end of the reaction period. During remelting (ROX3), the sources of oxygen are quite limited, so that further reaction is believed to be restricted. Finally, as reported by Mcleod in a study of the reaction between Mg and Al_2O_3,[34] MgO

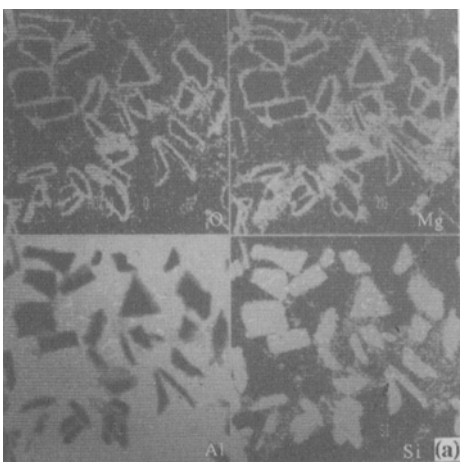

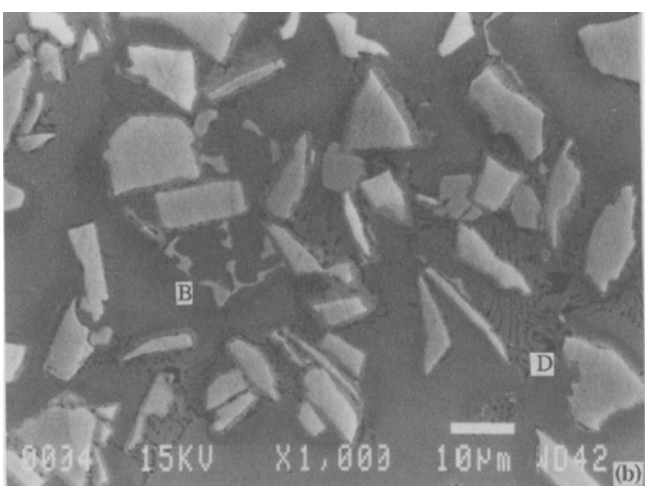

Fig. 14—(*a*) SEM X-ray maps showing the segregation of Mg, O at the interfaces. (*b* $(Cr,Mn,Fe)_3SiAl_{12}$ (B) and Mg_2Si (D) found in the matrix and near SiC*p* (AOX14).

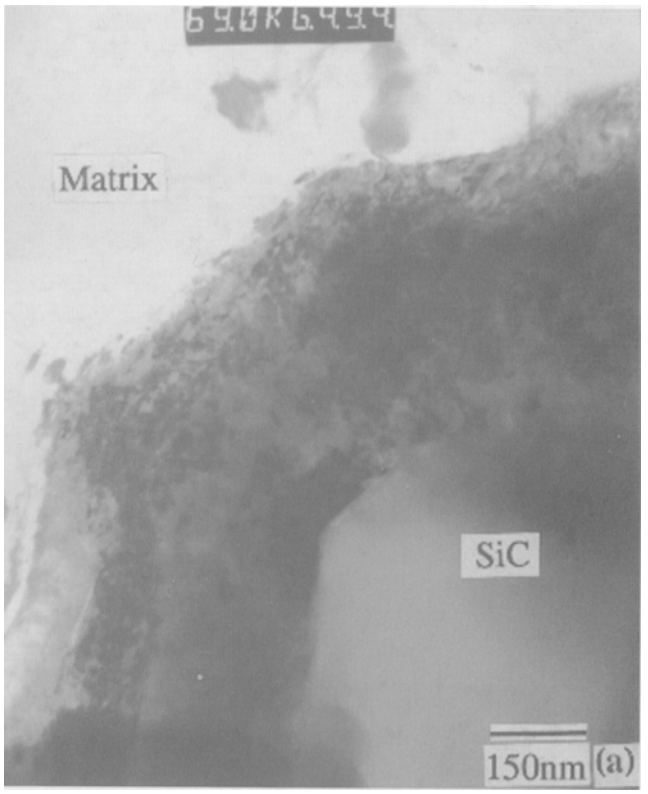

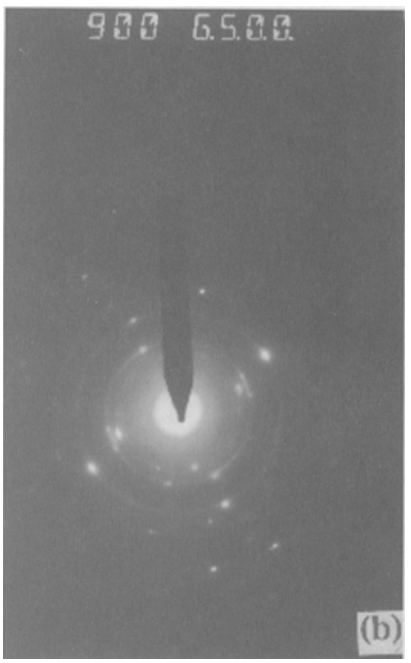

Fig. 15—(*a*) TEM BF image of the interface (AOX14). (*b*) SAD pattern with strong MgO rings.

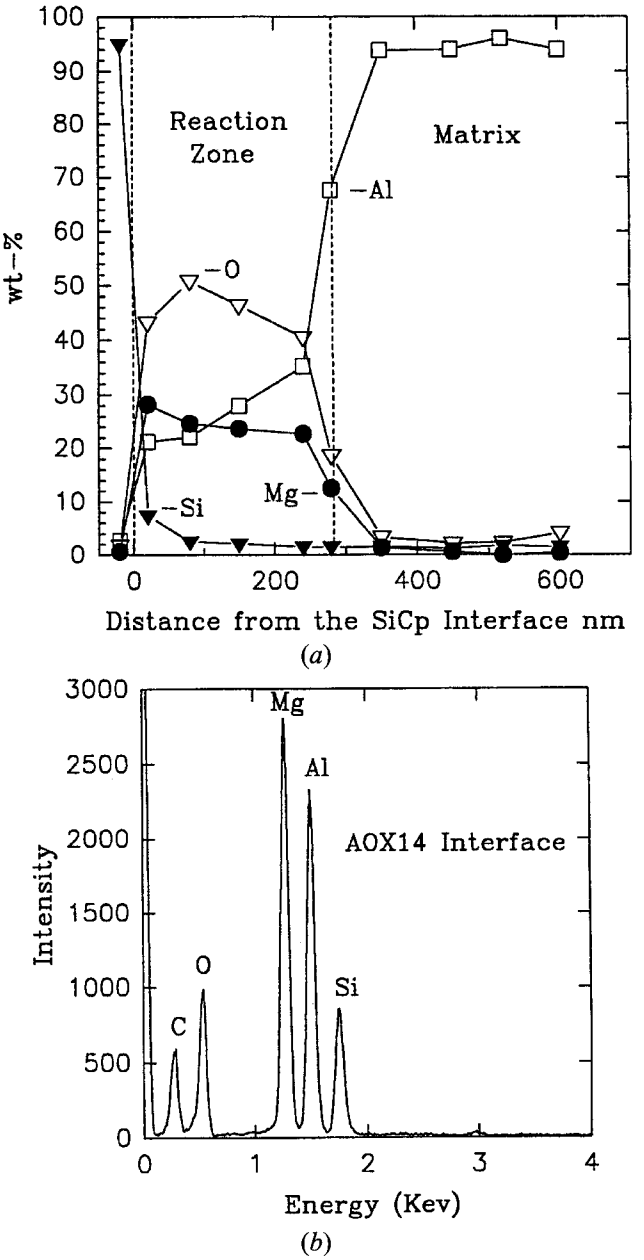

Fig. 16—(*a*) EDS concentration profile for AOX14. (*b*) EDS spectrum in the reaction zone.

is more stable than $MgAl_2O_4$ when the Mg content is larger than 1.6 wt pct at 800 °C. For our material, the remaining Mg content in the matrix is still as high as about 3 wt pct after fabrication, so that the reaction products could be unchanged during remelting. Considering the AOX14 sample, because the SiO_2 layer is thicker, the interfacial reaction during fabrication will consume much more Mg (more than 3 wt pct according to our measurements). The amount of Mg calculated based on Reactions [1] and [3], however, indicates that there should be no Mg remaining in the matrix if the interfacial reaction between SiO_2 and Mg went to completion and all of the released Si formed Mg_2Si after solidification. Thus, MgO can be formed at the beginning of the reaction, whereas with an increase of reaction time, the Mg level in the matrix will decrease significantly and some $MgAl_2O_4$ will be formed at interfaces. Since the liquid Mg content can be expected to be larger than the bulk Mg content during compocasting, as discussed previously, and the reaction between Mg and the SiO_2 layer is incomplete because of the short fabrication time, the amount of $MgAl_2O_4$ formed is limited during casting and MgO is the main reaction product. However, during remelting at 800 °C, the matrix is completely melted, so that the Mg content in the liquid is the same as that in the bulk at that time (the

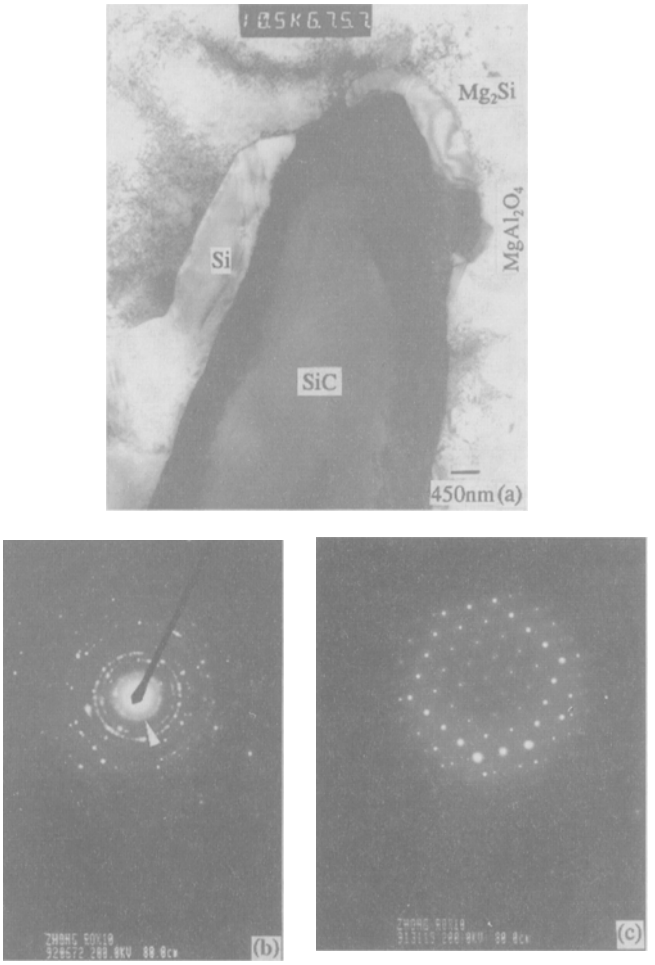

Fig. 17—(*a*) TEM BF image, Si, Mg_2Si, and $MgAl_2O_4$ observed near the reaction zone in the matrix. (*b*) SAD pattern from the reaction zone indicating very strong (111)spinel diffraction. (*c*) SAD pattern of B[110]$MgAl_2O_4$ (ROX14).

remaining Mg content in the matrix is less than 1 wt pct after fabrication). The interfacial reaction between Mg (Al) and SiO_2 during remelting will therefore mainly form $MgAl_2O_4$. In addition, in systems with a low Mg content, $MgAl_2O_4$ is more stable,[34] so that some of the MgO initially formed could be transformed to $MgAl_2O_4$ during remelting. In order to understand more fully the relation between the amount of MgO (or $MgAl_2O_4$) formed as a result of the interfacial reaction and the thickness of the SiO_2 layer during fabrication, thermodynamic calculations were carried out for a given system using the F*A*C*T Thermodynamic Database.[35] As shown in Figure 20 and Table I, the possibility of forming $MgAl_2O_4$ increases with increasing thickness of the SiO_2 layer for a given alloy composition (assuming an uniform distribution of Mg). It therefore appears that a detailed discussion of interfacial reactions in composites requires consideration not only of the matrix composition but also of the type, volume fraction, and size of the reinforcement in addition to the thickness of coatings (if present).

Since MgO is expected to form first and $MgAl_2O_4$ later in AOX14 samples, the distribution of MgO and $MgAl_2O_4$ will not be uniform and there should be more MgO in the outer layer of the reaction zone and more $MgAl_2O_4$ in the inner layer of the reaction zone. However, because of the limited size of the objective aperture, it is not possible to select diffraction spots which originate uniquely from MgO or $MgAl_2O_4$ crystals so that TEM DF images, which uniquely consist of MgO crystals or $MgAl_2O_4$ crystals, could not be obtained to visualize their spatial distribution. In addition, because the reaction is controlled by a short-circuit diffusion, the reaction front will not necessarily move uniformly inside the reaction zone. Thus, in some areas, the reaction can occur deeply inside the reaction zone if the reaction in areas outside the reaction zone has not been completed. As a result, MgO and $MgAl_2O_4$ may form anywhere in the reaction zone.

V. CONCLUSIONS

1. In the as-cast composite materials, there is no attack of SiC*p* by molten Al whether or not the SiC*p* has been artificially oxidized.

(a) In as-cast composites reinforced with as-received SiC*p*, segregation of Mg at the matrix/SiC*p* interface is observed. Some of the Mg forms fine MgO crystals at the matrix/SiC*p* interface with a thickness of about 20 to 30 nm.

(b) In as-cast composites reinforced with 3.04 wt pct oxidized SiC*p* (AOX3) or with 14.06 wt pct oxidized SiC*p* (AOX14), a reaction layer consisting mainly of fine MgO crystals (5 to 20 nm) is found. This reaction layer has a straight, clear interface with the SiC particle and has an average thickness of 100 to 200 nm in the AOX3 sample and 500 to 800 nm in the AOX14 sample.

2. In remelted materials, different behaviors are found for different initial conditions of the SiC*p*.

(a) In RMS materials (as-received SiC*p*, remelted), SiC*p* is attacked heavily. MgO crystals formed during fabrication remain at the original interface position.

(b) In ROX3 material (3.04 wt pct oxidized SiC*p*, remelted), MgO is still the main reaction product in the reaction zone. In ROX14 materials (14.06 wt pct oxidized SiC*p*, remelted), the proportion of $MgAl_2O_4$ is increased at the interfaces. The type of reaction product formed is related to the dynamic concentration of Mg in the matrix. Attack of SiC*p* in ROX3 materials is observed only on some SiC*p* and the attack is slight. In ROX14 materials, the attack of SiC*p* is not observed. Attack of SiC by molten Al is decreased with increasing thickness of the SiO_2 layer. Mg_2Si, Si, and $(Cr,Mn,Fe)_3SiAl_{12}$ are found in the matrix near the SiC particles.

3. The newly formed MgO (or spinel) crystal boundaries are believed to be the diffusion paths (or channels) for the interfacial reactions to proceed. Higher Mg concentrations in the matrix will result in a denser MgO reaction zone which may protect the SiC particles better than the $MgAl_2O_4$ reaction zone.

ACKNOWLEDGMENTS

The authors gratefully acknowledge the NATO International Scientific Exchange Programme (Grant No. CRG 900950) and the National Science and Engineering Council of Canada (NSERC, strategic grants) for financially supporting this project. They also thank E. Goiffon, L. Salvo, and J.J. Blandin for the preparation of the composite ma-

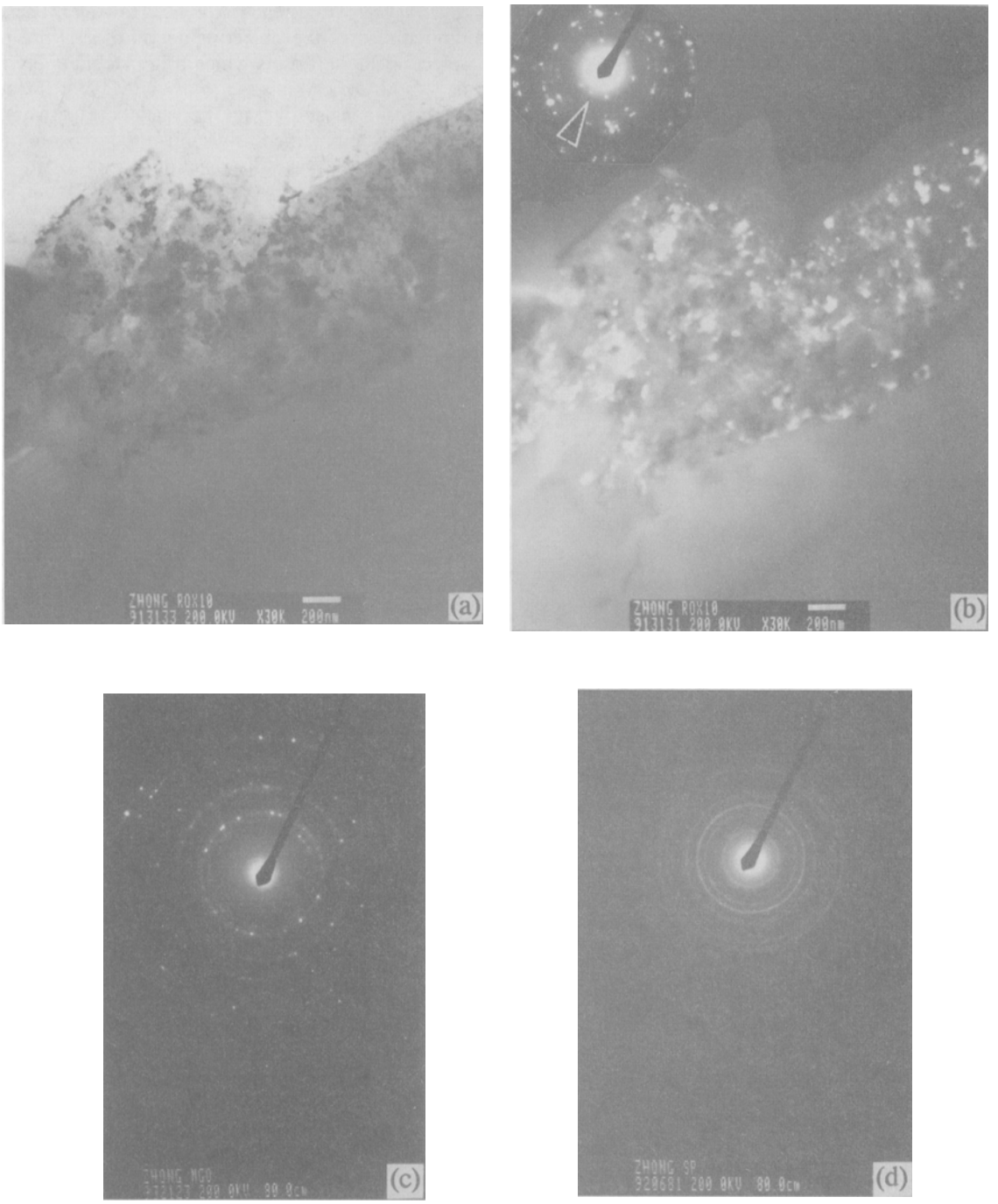

Fig. 18—(*a*) TEM BF image of the reaction zone around SiC*p*. (*b*) DF image by (111)spinel in ROX14 sample and diffraction patterns of (*c*) pure MgO and (*d*) pure $MgAl_2O_4$.

terials. Thermodynamic calculations were performed with the help of P. Wu and J. Wu.

REFERENCES

1. L. Salvo, M. Suéry, J.G. Legoux, and G. L'Espérance: *Mater. Sci. Eng.*, 1991, vol. A135, p. 129.
2. H. Ribes, R.Da. Silva, M. Suéry, and T. Bretheau: *Mater. Sci. Technol.*, 1990, vol. 6, p. 621.
3. F. Delannay, L. Froyen, and A. Deruyttere: *J. Mater. Sci.*, 1987, vol. 22, p. 1.
4. C. Marumo and J.A. Pask: *J. Mater. Sci.*, 1977, vol. 12, p. 223.
5. J.G. Legoux, H. Ribes, G. L'Espérance, and M. Suéry: *Proc. Interfaces in Metal-Ceramics Composites*, Anaheim, 1989, R.Y. Lin and R.J. Arsenault, G.P. Martins and S.G. Fishman, eds. (The Minerals, Metals & Materials Society, 1989, p. 187)
6. D.J. Lloyd, H. Lagace, A. McLeod, and P.L. Morris: *Mater. Sci. Eng.*, 1989, vol. A107, p. 73.
7. F.H. Samuel, H. Liu, and A.M. Samuel: *Metall. Trans. A*, 1993, vol. 24A, pp. 1631-45.
8. J. Narciso, C. Garcia-Cordovilla, and E. Louis: *Mater. Sci. Eng.*, 1992, vol. B15, p. 148.
9. J.G. Legoux, G. L'Espérance, L. Salvo, and M. Suéry: *Proc. Fabrication of Particulates Reinforced Metal Composites*, Montreal,

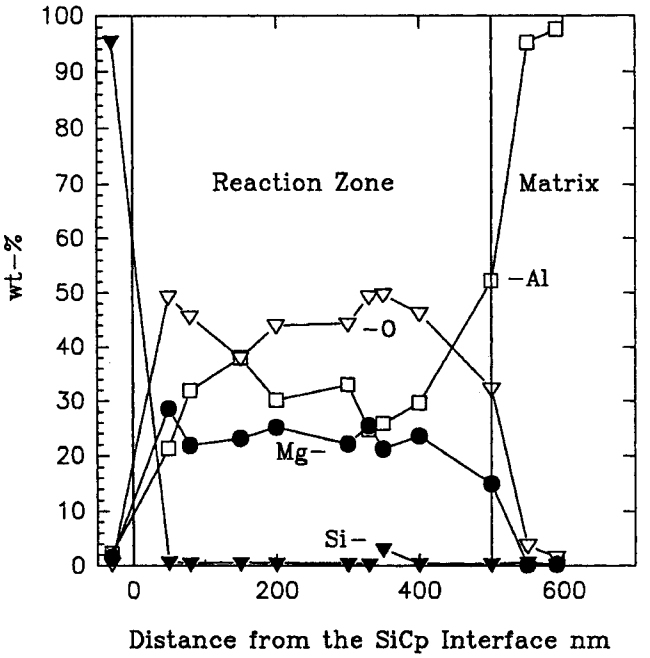

Fig. 19—EDS profile at matrix/SiC*p* interface (ROX14).

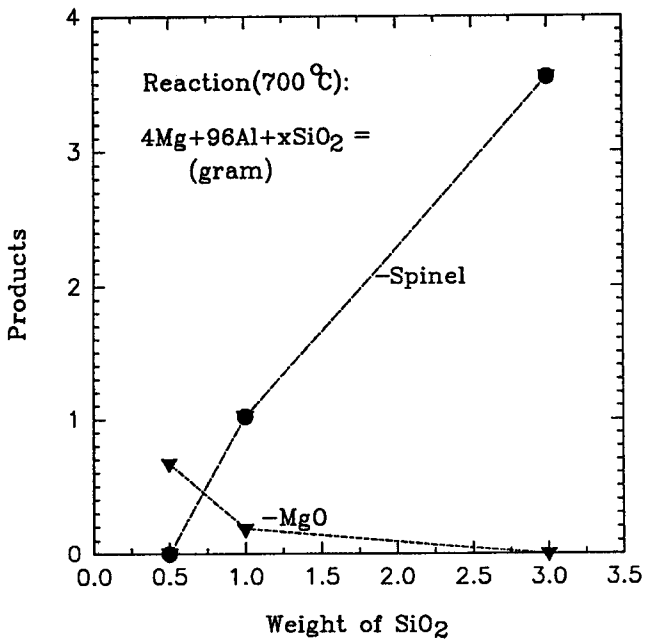

Fig. 20—Effect of SiO_2 on the interfacial reaction products.

Table I. Relation between the Reaction Products and the Amount of SiO_2

Products	$0.5SiO_2$ (R1)*	$1.0SiO_2$ (R2)	$3.0SiO_2$ (R3)
MgO	0.671	0.184	0.000
$MgAl_2O_4$	0.000	1.021	3.552
Mg_2Si	0.638	1.277	2.213
Si	0.000	0.000	0.592
SiO_2 (rest)	0.000	0.000	0.000
Mg (rest)	3.149	2.832	1.860

*Calculations using the F*A*C*T Thermodynamic Database[35] at 700 °C, 1 atm, in grams. R1, R2, and R3 indicate different reactions with different amounts of SiO_2**.

$$4Mg + 96Al + 0.5SiO_2 = [R1]$$
$$4Mg + 96Al + 1.0SiO_2 = [R2]$$
$$4Mg + 96Al + 3.0SiO_2 = [R3]$$

**In the AOX3 sample (with 3.04 wt pct SiO_2), there is 0.65 g SiO_2 per 100 g of matrix, which is similar to condition R1. In the AOX14 sample (with 14.06 wt pct SiO_2), there is 2.94 g SiO_2 per 100 g of matrix, which is similar to condition R3.

1990, J. Masounave and F.G. Hamel, eds., p. 31. (ASM, Metals Park, Ohio, 1990)
10. D.J. Lloyd and I. Jin: *Metall. Trans. A*, 1988, vol. 19A, pp. 3107-09.
11. C.A. Handwerker, J.W. Cahn, and J.R. Manning: *Mater. Sci. Eng.*, 1990, vol. A126, p. 173.
12. J.C. Viala, P. Fortier, and J. Bouix: *J. Mater. Sci.*, 1990, vol. 25 (3), p. 1842.
13. T. Iseki, T. Kameda, and T. Maruyama: *J. Mater. Sci.*, 1984, vol. 19, p. 1692.
14. K.J. Brondyke: *J. Am. Ceram. Soc.*, 1953, vol. 36 (5), p. 171.
15. T. Stephenson, Y. Le Petitcorps, and J.M. Quenisset: *Mater. Sci. Eng.*, 1991, vol. 135A, p. 101.
16. I. Jin and D.J. Lloyd: *Proc. 2nd Int. Conf. on Cast Metal Matrix Composites*, Tuscaloosa, AL, Oct. 1993, D.M. Stefanescu and S. Sen, eds., p. 288. American Foundrymen's Soc. Inc., Illinois, 1994.
17. E. Goiffon, W. Zhong, J.J. Blandin, M. Suéry, and G. L'Espérance: *Proc. 2nd Int. Conf. on Cast Metal Matrix Composites*, Tuscaloosa, AL, Oct. 1993, D.M. Stefanescu and S. Sen, eds., pp. 316-25. (ibid 16)
18. W.M. Zhong and G. L'Espérance: University of Montreal, Montreal, unpublished research, 1993.
19. R.Y. Lin and K. Kannikeswaran: *Proc. Interfaces in Metal-Ceramics Composites*, Anaheim, CA, 1989, R.Y. Lin and R.J. Arsenault, eds., p. 153. (ibid 5)
20. K. Kannikeswaran and R.Y. Lin: *J. Met.*, 1987, vol. 9, p. 17.
21. D.J. Lloyd and B. Chamberlain: *Proc. Interfaces in Metal-Ceramics Composites*, Anaheim, CA, 1989, R.Y. Lin and R.J. Arsenault, eds., p. 263. (ibid 5)
22. G. Selvaduray, R. Hickman, D. Quinn, D. Richard, and D. Rowland: *Proc. Interfaces in Metal-Ceramics Composites*, Anaheim, CA, 1989, R.Y. Lin and R.J. Arsenault, eds., p. 271. (ibid 5)
23. M. Strangewood, C.A. Hippley, and J.J. Lewandowski: *Scripta Metall.*, 1990, vol. 24, p. 1483.
24. A. Munitz, M. Metzger, and R. Mehrabian: *Metall. Trans. A*, 1979, vol. 10A, pp. 1491-97.
25. M. Fishkis: *J. Mater. Sci.*, 1991, vol. 261, p. 2651.
26. T. Malis and M.C. Chaturvedi: *J. Mater. Sci.*, 1982, vol. 17, p. 1479.
27. L.M. Dignard-Bailey, T.F. Malis, J.D. Boyd, and J.D. Embury: *CIM Proc.*, 1988, vol. 9, p. 87.
28. A. Mortensen: *Mater. Sci. Eng.*, 1991, vol. A135, p. 1.
29. A. Mortensen, J.A. Cornie, and M.C. Flemings: *J. Met.*, 1988, vol. 2, p. 12.
30. B. Hallestedt, Z.K. Liu, and J. Agren: *Mater. Sci. Eng.*, 1990, A129, p. 135.
31. J. Horváth: *Defect Diffus. Forum*, 1989, vols. 66–69, p. 207.
32. B.S. Bokstein: *Defect Diffus. Forum*, 1989, vol. 66–69, p. 631.
33. W.M. Zhong, G. L'Espérance, and M. Suéry: University of Montreal, Montreal, unpublished research, 1993.
34. A.D. Mcleod: *Proc. Fabrication of Particulates Reinforced Metal Composites*, Montreal, 1990, J. Masounave and F.G. Hamel, eds., p. 18. (ibid 9)
35. *F*A*C*T Thermodynamic Database*, CRCT, Ecole Polytechnique, Montreal, 1993.